International Research Journal of Engineering and Technology (IRJET) e-ISSN: 2395-0056
Volume: 07 Issue: 09 | Sep 2020 www.irjet.net p-ISSN: 2395-0072

Numerical Analysis of the Three-Dimensional Aerodynamics of a Thrush Nightingale (Luscinia Luscinia)

Kunal Ghosh

Student, Dept. of Aerospace Engineering and Applied Mechanics, IIEST, Shibpur, Howrah, West Bengal, India

---

Abstract – *The present study is devoted to estimate the amount of lift and drag produced by the Thrush Nightingale in a steady flight using CFD (Computational Fluid Dynamics). The DPIV (digital particle image velocimetry) data of the flight of thrush nightingale is used to track the flapping mechanism of the bird. The present study is done using an overset meshing technique to simulate the flapping of the wings, which is computationally much cheaper than most of is its counterparts like remeshing of the computational domain. The corresponding lift and drag generated by the bird during steady flight at 10m/s are obtained from this study. It's found similar to most of the other birds, i.e. most of the lift is being produced during the downstroke of the flaps. This study is done in ANSYS Fluent 19.2.*

Key Words: **Flapping wing, CFD, Wingbeat kinematics, aerodynamics, Thrush Nightingale (Luscinia *luscinia)*, Overset meshing, Lift, Drag.**

1. INTRODUCTION

The flapping wing mechanism has gained very wide popularity in recent years. While different species of hummingbirds are very extensively studied by the researchers, other birds like the thrush nightingale, have many not gained so much popularity. In the recent past, many researchers are getting interested in these amazing creatures and their equally amazing flight mechanisms. Though the seemingly simple and monotonous flapping wing mechanism is not something new, it is something that is yet to be fully explored. The increasing popularity of the ornithopter is encouraging the researchers to investigate the flapping wings further. Ornithopters have numerous advantages over conventional aircrafts and rotorcrafts. They are way more maneuverable and consume much less energy. These advantages can be exploited best at small sizes and the low speeds which are most suitable for several applications like search operations and delivery of small packages to name a few.

In this study, we have used the PIV data obtained by Rosen et al. [1] for wing kinematics of the flapping mechanism. We have considered the body of the bird to be stationary. The stability of the flight is not studied in the present work. So the tail is assumed to be stationary in this work. The body of the bird is assumed to be axis-symmetric except for the tail part of it. The wing is placed a little far away from the body of the bird to mesh it properly using overset meshing. Both the body of the bird and the wings are considered as rigid bodies in this study, though real thrush nightingale is not rigid and there are some fluid-structure interactions. Unlike most of the previous studies, we have assumed a finite thickness to the wings i.e. 2mm. The three-dimensional model of the bird is prepared in SolidWorks.

2. LITERATURE REVIEW

The relationship between wingbeat kinematics and vortex wake of a thrush nightingale (*Luscinia luscinia*) was extensively studied by M. Rosén, G. R. Spedding, and A. Hedenström [1]. They have provided an analytical relation between the stroke angle and the time in an individual flap for a number of the flight speeds ranging from 5 to 10 m/s. These relations are used in this study to simulate the flapping of the wings of the bird in the present study. Wingbeat frequency and the body drag anomaly of thrush nightingale and a teal (*Anas crecca*) is studied by C. J. Pennycuick, Marcel Klaassen, Anders Kvist, and Åke Lindström [2].

Three-dimensional aerodynamics of a hovering rufous hummingbird (*Selasphorus rufus*) is studied numerically by Songyuan Yang and Weiping Zhang [3], where they have placed the wing little away from the body of the bird.

3. COMPUTATIONAL DOMAIN

The computational domain is chosen to be a hemispherical one for the background mesh, with only half of the geometry as shown in fig. 2 along with a single wing enclosed within a sphere as shown in fig. 3. This is done to reduce the computational cost of this study. We have used the diameter of the sphere about 20 times the length of the body of the bird. Overset meshing is used in this study for the motion of the wings. Tetrahedral elements are used to mesh both of the computational domains. At the interface of the overset, we have used the smoothing functionality of the fluent. The reason behind choosing smoothing over the more accurate remeshing is that of the huge computational cost associated with remeshing. We have chosen the size of the elements from 40mm to 0.1 mm, in this study. Also, 5 layers of inflation are created on both the body and the wing to capture the boundary layer properly. Inflation layers are also set as a rigid body along with the body of the bird and the wing i.e. we are keeping the mesh in the inflation layer unaltered throughout the study. The body of the bird and wing is set as walls, while the curved surface is shown in fig. 2(a) is set as a velocity

inlet with 10m/s speed in the negative x-direction. The spherical surface is shown in fig. 3 is set as an overset interface.

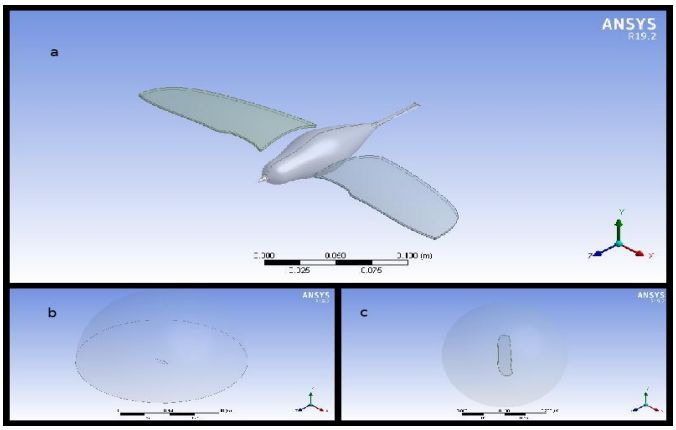

Fig -1: Geometry of the bird

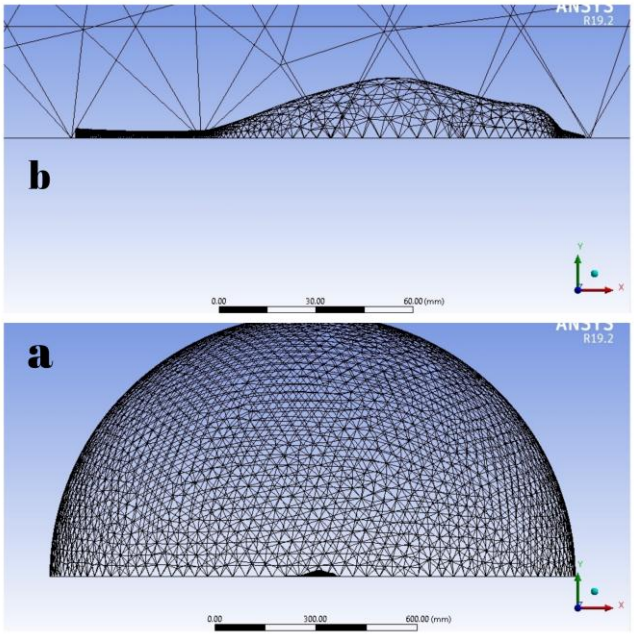

Fig -2: Background Mesh

a. Total coputational domain

b. Body of the bird

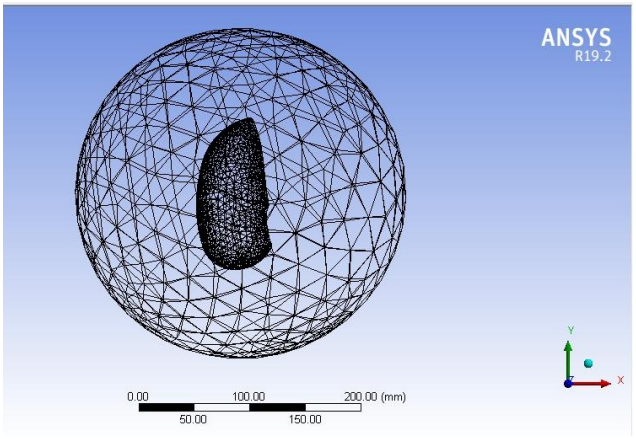

Fig -3: Moving Mesh

4. THEORY

In the present work, the Navier Stokes Equation is solved numerically using a commercial CFD code (ANSYS FLUENT). It uses the finite volume method to solve the Navier Stokes Equation. For the turbulence modeling, we have used the $k-\omega$ SST model as done in many of the previous studies, which is a RANS (Reynolds Average Navier Stokes) turbulence model.

RANS Equations:

Continuity Equation:

$$\frac{\partial u_i}{\partial x_i} = 0$$

Momentum Equation :

$$\rho\frac{\partial U_i}{\partial t} + \rho U_j\frac{\partial U_i}{\partial x_j} = -\frac{\partial P}{\partial x_i} + \frac{\partial}{\partial x_j}((2\mu S_{ji}) - (\rho\overline{u_j'u_i'}))$$

where,

$$s_{ij} = \frac{1}{2}((\frac{\partial u_i}{\partial x_j}) + (\frac{\partial u_j}{\partial x_i}))$$

and for any quantity let 'a' in the above equations we use the following notations :

a = A + a'

Quantity = Average Value + Perturbation

Transport Equations:

$$\frac{\partial}{\partial t}(\rho k) + \frac{\partial}{\partial x_i}(\rho k u_i) = \frac{\partial}{\partial x_j}(\Gamma_k\frac{\partial k}{\partial x_j}) + G_k - Y_k + S_k$$

$$\frac{\partial}{\partial t}(\rho\omega) + \frac{\partial}{\partial x_j}(\rho\omega u_j) = \frac{\partial}{\partial x_j}(\Gamma_\omega \frac{\partial \omega}{\partial x_j}) + G_\omega - Y_\omega + S_\omega$$

where,

u_i *= Velocity along i th direction*

P = Pressure

$\rho = Density$

k = Turbulence Kinetic Energy

ω *= Specific dissipation rate*

$\Gamma_i =$ *Effective diffusivity of i*

G_i *= Generation of i due to mean velocity*

Y_i *= Dissipation of i due to turbulence*

S_i *= User defined source terms of i*

5. WING KINEMATICS

Equations of motion used in this study are derived from the data obtained by Rosen et al. [1]. The periodic nature of the flapping mechanism inspires us to use fourier transform to model the flapping of the wing from fig. 4 of Rosen et al. [1]. The curve fitting is done using the Curve Fitting Toolbox of MATLAB. Velocity is evaluated by differentiating the angular displacements obtained. We have divided a single flap into 70 steps each of 0.001s totaling to 0.070s for each of the individual flaps. We have assumed the flow to be uniform in the negative x-direction with a magnitude of 10m/s. Also as the fluent follows the transformation as ZXY, so we have to transform all the angular velocities accordingly to get the appropriate motions as shown:

$$Z = \begin{bmatrix} cos(\psi) & -sin(\psi) & 0 \\ sin(\psi) & cos(\psi) & 0 \\ 0 & 0 & 1 \end{bmatrix}$$

$$X = \begin{bmatrix} 1 & 0 & 0 \\ 0 & cos(\phi) & -sin(\phi) \\ 0 & sin(\phi) & cos(\phi) \end{bmatrix}$$

$$Y = \begin{bmatrix} cos(\theta) & 0 & sin(\theta) \\ 0 & 1 & 0 \\ -sin(\theta) & 0 & cos(\theta) \end{bmatrix}$$

$$\dot{\vec{\psi}} = \begin{bmatrix} 0 \\ 0 \\ \dot{\psi} \end{bmatrix}$$

$$\dot{\vec{\phi}} = \begin{bmatrix} \dot{\phi} \\ 0 \\ 0 \end{bmatrix}$$

$$\dot{\vec{\theta}} = \begin{bmatrix} 0 \\ \dot{\theta} \\ 0 \end{bmatrix}$$

$$\vec{\omega} = (YX\dot{\vec{\psi}}) + (Y\dot{\vec{\phi}}) + (\dot{\vec{\theta}})$$

$$\vec{\omega} = \begin{bmatrix} (\dot{\phi}cos(\theta)) + (\dot{\psi}cos(\phi)sin(\theta)) \\ \dot{\theta} - (\dot{\psi}sin(\phi)) \\ (\dot{\psi}cos(\theta)cos(\phi)) - (\dot{\phi}sin(\theta)) \end{bmatrix}$$

where,

$$\omega = 89.7597901$$

$$\phi = A_0 + (A_1 cos((t + 0.033)\omega)) + (B_1 sin((t + 0.033)\omega))$$

$$\dot{\phi} = B_1\omega cos((t + 0.033)\omega) - A_1\omega sin((t + 0.033)\omega)$$

A_0 *= -0.1287,* A_1 *= -0.0001445,* B_1 *= 0.642*

$$\psi = a_0 + a_1 cos((t + 0.033)\omega) + b_1 sin((t + 0.033)\omega) + a_2 cos(2(t + 0.033)\omega) + b_2 sin(2(t + 0.033)\omega)$$

$$\dot{\psi} = b_1\omega cos((t + 0.033)\omega) + 2b_2\omega cos(2(t + 0.033)\omega) - a_1\omega sin((t + 0.033)\omega) - 2a_2\omega sin(2(t + 0.033)\omega)$$

a_0 *= 0.8985,* a_1 *= 0.4781,* b_1 *= -0.2094,*b_2 *= 0.06621,* a_2 *= -0.2094*

$$\theta = 0$$

$$\dot{\theta} = 0$$

This is the angular velocity we will be using to calculate the motion of the wings.

(All the stroke angle is shown in fig. 4 and fig. 5 is measured relative to the body axis which in this case is also the same as the global coordinate system. Also, the angle between the wing and the yz-plane as shown in fig. 5 is measured relative to the body axis which in this case is again the global coordinate system.)

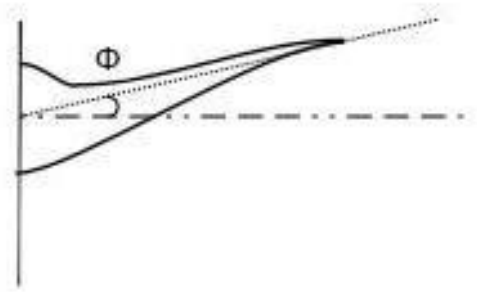

Fig -4: $\phi Angle$

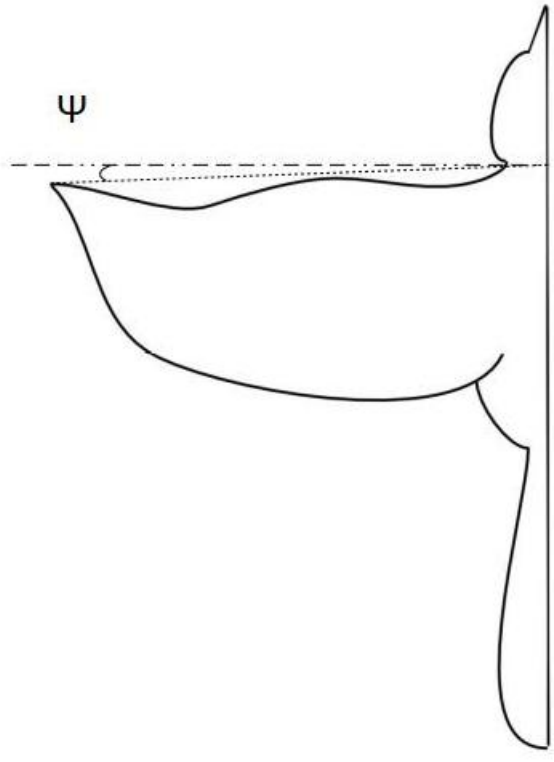

Fig -5: $\psi Angle$

The UDF (User Defined Function) used for the motion is shown in the fig. 6

```
#include "udf.h"
#define pi 3.141592653589793

real phi,psi;
real phidot,psidot;
real x = 0.0;
real tau = 0.07; // time period of 1 flap
real t = 0.0; // time
real a0 = 0.8985;
real a1 = 0.4781;
real b1 = -0.2094;
real a2 = -0.2094;
real b2 = 0.06621;
real w = 89.7597901; // Circular frequency
real A0 = -0.1287;
real A1 = -0.0001445;
real B1 = 0.642;

DEFINE_CG_MOTION(flapping,dt,vel,omega,time,dtime)

{
x = time+0.033;

psi = a0 + a1*cos(x*w) + b1*sin(x*w) + a2*cos(2*x*w) + b2*sin(2*x*w);

psidot = b1*w*cos(w*x) + 2*b2*w*cos(2*w*x) - a1*w*sin(w*x) - 2*a2*w*sin(2*w*x);

phi = A0 + A1*cos(x*w) + B1*sin(x*w);

phidot = B1*w*cos(w*x) - A1*w*sin(w*x);

vel[0] = 0.0;  // x-velocity
vel[1] = 0.0;  // y-velocity
vel[2] = 0.0; // z-velocity

omega[0] = phidot;  // x-angular velocity
omega[1] = -psidot*sin(phi); // y-angular velocity
omega[2] = psidot*cos(phi); // z-angular velocity

}
```

Fig -6: UDF

The variation of ϕ and ψ with time is shown in the fig. 7. The angular velocities $\dot{\phi}$ and $\dot{\psi}$ is obtained by differentiating the corresponding angles, shown in the fig. 8.

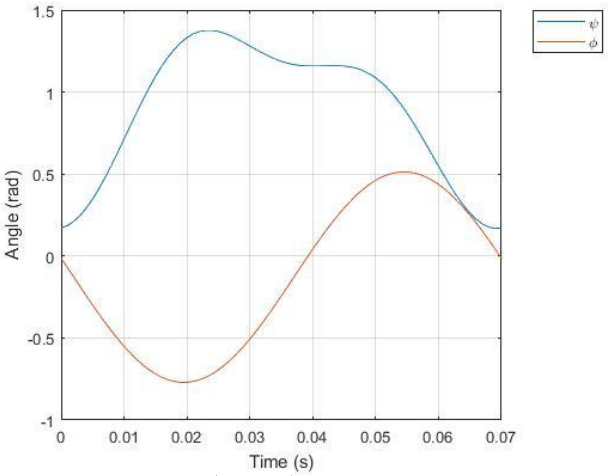

Fig -7: ϕ and ψ variation with time

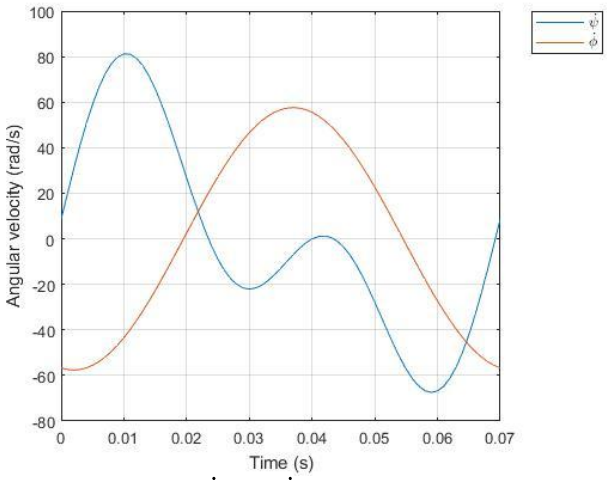

Fig -8: $\dot{\phi}$ and $\dot{\psi}$ variation with time

6. RESULTS

In this study, the flow is assumed to be an incompressible one. All the results shown in this study are converged to 10e-4 accuracy of the residuals. Roe-FDS scheme is used in this simulation. The contour plot of the velocity and the pressure over the body of the bird and the wing is shown in fig. 9 and fig. 10, respectively.

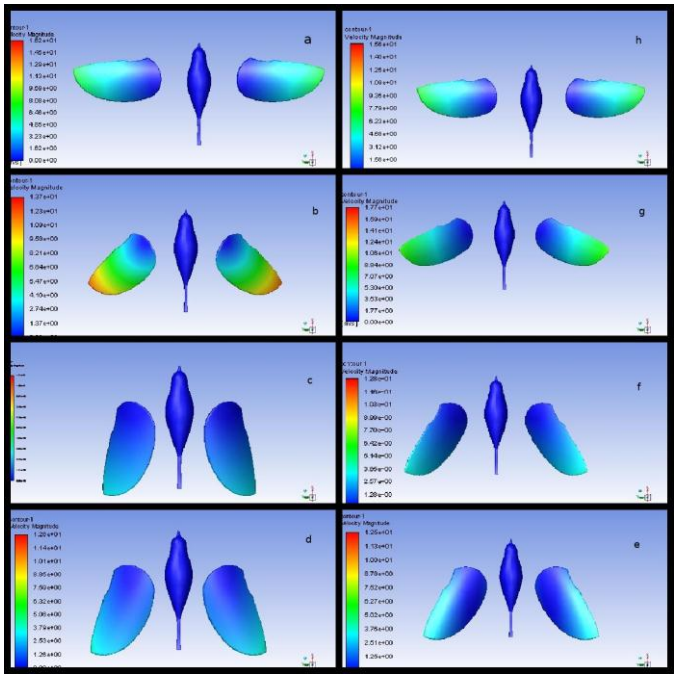

Fig -9: Velocity contour over the wing and the body of the bird.

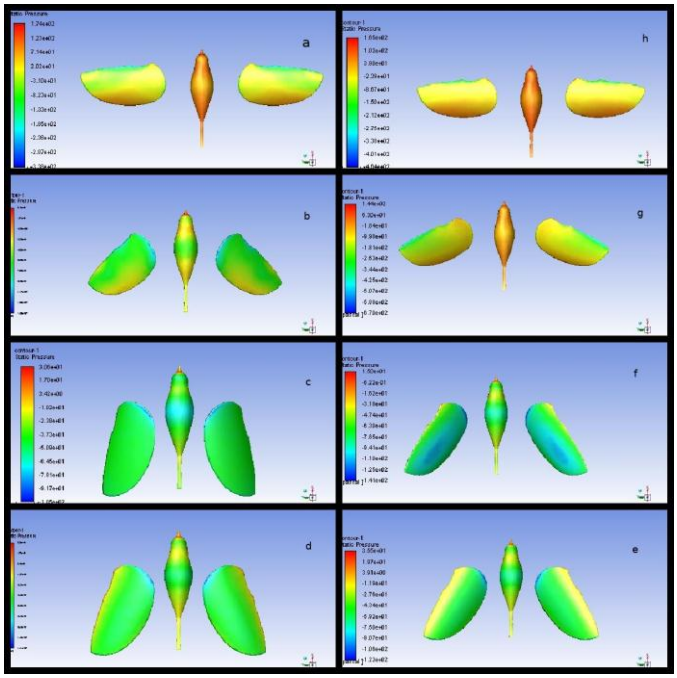

Fig -10: Velocity contour over the wing and the body of the bird.

The variation of the lift is shown in fig. 11. It can be seen from fig. 11 that the major amount of the lift is produced during the downstroke. Though there is a smaller peak in the upstroke, the major amount of the lift produced during the downstroke of the flap.

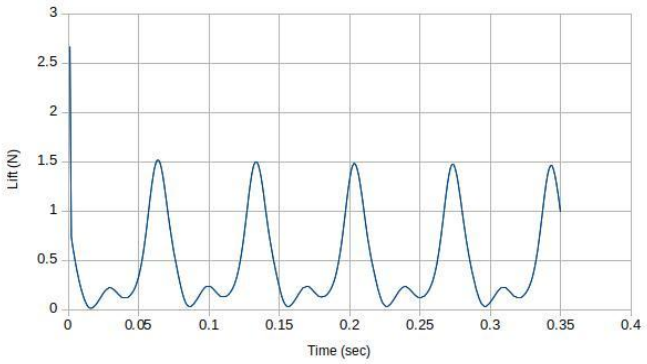

Fig -11: Variation of the lift with time

The variation of the drag is shown in fig. 12. Unlike the variation of the lift, there is only a single peak during the downstroke of the flap.

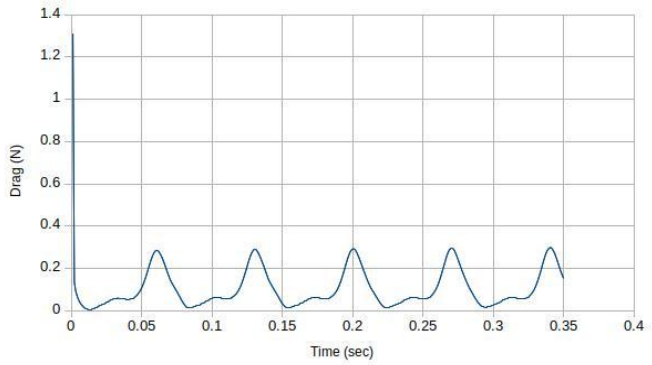

Fig -12: Variation of the drag with time

7. CONCLUSIONS

We have simulated 5 flaps and the lift and drag produced are found to follow almost similar patterns except for the first flap in which the initial time step is producing abnormally high lift and drag.

The peak of the lift and drag is found to occur at almost the same time step during the downstroke of the flap. As shown in fig. 13 most of the lift is produced during the last part of the flap when the downstroke just started to begin in a flapping cycle.

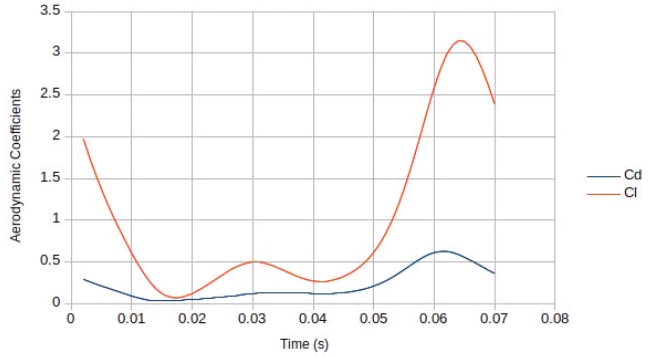

Fig -13: Cl and Cd variation with time

where,

$C_L = \frac{L}{0.5\rho v^2 S}$ (Coefficient of lift)

$C_D = \frac{D}{0.5\rho v^2 S}$ (Coefficient of drag)

$\rho = 1.225 kg/m^3$ (Density)

$v = 10 m/s$ (Free stream velocity)

$S = 0.0076657 m^2$ (Projected area of the wing)

The average amount of the lift produced during these 5 flaps is estimated to be 0.4731 N in each flap. While the approximate weight of a typical thrush nightingale is about 0.2943 N (mass is about 30 gm). So, it can easily support its weight. We have placed the wing a little far away from the body as shown in fig. 1, so the interference effect of the body is not properly accounted. Moreover, the lift and drag characteristics of the tail are entirely neglected which do have a significant contribution to the stability of the flight.

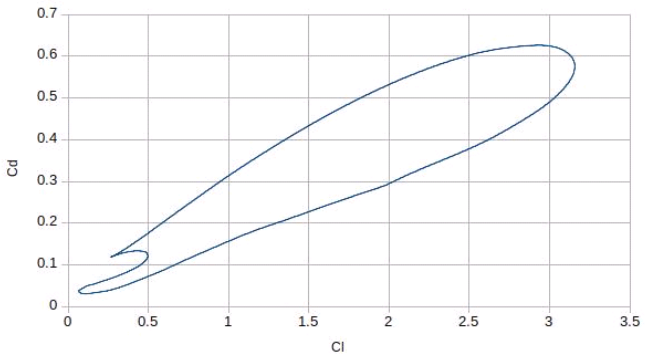

Fig -14: Drag Polar

The drag polar of the flapping wing is depicting a very sharp edge as shown in the fig. 14. This can be correlated to fig. 10 (f) where we can see the flow separation in the form of the low-pressure regions.

ACKNOWLEDGEMENT

This study is impossible without the excellent softwares from the Ansys® Fluent, SolidWorks and MATLAB.

REFERENCES

[1] M. Rosén, G.R. Spedding and A. Hedenström, "The relationship between wingbeat kinematics and vortex wake of a thrush nightingale" The Journal of Experimental Biology 2004 207, Published by The Company of Biologists 2004 , pp. 4255-4268, doi:10.1242/jeb.01283.

[2] C J Pennycuick, M Klaassen, A Kvist and Å Lindström, "Wingbeat frequency and the body drag anomaly: wind-tunnel observations on a thrush nightingale (Luscinia luscinia) and a teal (Anas crecca)" The Journal of Experimental Biology 1996 199, Published by The Company of Biologists Limited 1996 , pp. 2757–2765.

[3] S. Yang, S. Zhang,"Numerical analysis of the three-dimensional aerodynamics of a hovering rufous hummingbird (Selasphorus rufus)". Acta Mech. Sin. 31, 2015, pp. 931–943. doi: 10.1007/s10409-015-0450-5

[4] G.R. Spedding, M. Rosén and A. Hedenström, "A family of vortex wakes generated by a thrush nightingale in free flight in a wind tunnel over its entire natural range of flight speeds" The Journal of Experimental

Biology 2003 206, Published by The Company of Biologists Ltd, pp. 2313-2344, doi:10.1242/jeb.00423.

[5] M. V. Cook, "Flight Dynamics Principles" Elsevier Ltd., 2007

[6] Tyson L. Hedrick , Bret W. Tobalske and Andrew A. Biewener "Estimates of circulation and gait change based on a three-dimensional kinematic analysis of flight in cockatiels (Nymphicus hollandicus) and ringed turtle-doves (Streptopelia risoria)" The Journal of Experimental Biology 2002 205, Published by The Company of Biologists Limited pp. 1389–1409.

[7] A. Hedenström, L. van Griethuijsen, M. Rosén and G.R. Spedding "Vortex wakes of birds: recent developments using digital particle image velocimetry in a wind tunnel" Animal Biology , Vol. 56, No. 4, 2006, pp. 535-549.

[8] M.R.M. Nawi and M.S.A. Azhar "Aerodynamics Performance of Barn Swallow Bird at Top Speed: A Simulation Study" Journal of Mechanical Engineering Vol SI 5(5), 2018, pp. 1-15.

[9] Z. Liang and H. Dong "Computational Analysis of Hovering Hummingbird Flight" 48th AIAA Aerospace Sciences Meeting Including the New Horizons Forum and Aerospace Exposition, Orlando, Florida, 4 - 7 January 2010.

[10] MATLAB R2017a and Curve Fitting Toolbox 3.5.5 Release 2019a, The MathWorks, Inc., Natick, Massachusetts, United States.

[11] Ansys® Fluent, Release 19.2,

[12] SolidWorks 2016